π–Conjugated Donor–Acceptor Copolymers Constituted of π–Excessive and π–Deficient Arylene Units. Optical and Electrochemical Properties in Relation to CT Structure of the Polymer

12 AUTHORS, INCLUDING:

Takaki Kanbara
University of Tsukuba
201 PUBLICATIONS **3,711** CITATIONS

Takashi Fukuda
National Institute of Advanced Industrial Sci…
140 PUBLICATIONS **2,257** CITATIONS

π-Conjugated Donor−Acceptor Copolymers Constituted of π-Excessive and π-Deficient Arylene Units. Optical and Electrochemical Properties in Relation to CT Structure of the Polymer

Takakazu Yamamoto,*,[†] Zhen-hua Zhou,[†] Takaki Kanbara,[†] Masaki Shimura,[†] Kenichi Kizu,[†] Tsukasa Maruyama,[†] Yoshiyuki Nakamura,[†] Takashi Fukuda,[†] Bang-Lin Lee,[†] Naoki Ooba,[‡] Satoru Tomaru,[‡] Takashi Kurihara,[‡] Toshikuni Kaino,[‡] Kenji Kubota,[§] and Shintaro Sasaki[‖]

Contribution from the Research Laboratory of Resources Utilization,
Tokyo Institute of Technology, 4259 Nagatsuta, Midori-ku, Yokohama 226, Japan,
NTT Opto-electronics Laboratories, Nippon Telegraph and Telephone Corporation,
Naka-gun, Ibaraki 319-11, Japan, Fuculty of Engineering, Gunma University, Tenjincho,
Kiryu 376, Japan, and School of Material Science, Japan Advanced Institute of Science and
Technology, 1-1 Asahidai, Tatsunokuchi, Ishikawa 923-12, Japan

Received May 9, 1996[⊗]

Abstract: Various π-conjugated copolymers constituted of π-excessive thiophene, selenophene, or furan units (Ar) and π-deficient pyridine or quinoxaline (Ar′) units have been prepared in high yields by the following organometallic polycondensation methods: (i) n X−Ar−Ar′−X + n Ni(0)Lm → (Ar−Ar′)$_n$ (X = halogen, Ni(0)-Lm = zerovalent nickel complex), (ii) n X−Ar−X + n Me₃Sn−Ar′−SnMe₃ → (Ar−Ar′)$_n$ (palladium catalyzed), and (iii) a X−Ar−X + b X−Ar′−X + (a + b)Ni(0)Lm → (Ar)$_x$(Ar′)$_y$. Powder X-ray diffraction analysis confirms an alternative structure of a polymer prepared by the method ii. The copolymers have a molecular weight of 5.4×10^3 to 3.3×10^5 and an [η] value of 0.37 to 4.4 dL g^{-1}. π−π* absorption bands of the copolymers generally show red shifts from those of the corresponding homopolymers, (Ar)$_n$ and (Ar′)$_n$, and the red shifts are accounted for by charge-transferred CT structures of the copolymers. For example, an alternative copolymer of thiophene and 2,3-diphenylquinoxaline gives rise to an absorption band at λ_{max} = 603 nm, whereas homopolymers of thiophene and 2,3-diphenylquinoxaline exhibit absorption peaks at about 460 and 440 nm, respectively. The CT copolymers are electrochemically active in both oxidation and reduction regions, showing oxidation (or p-doping) peaks in a range of 0.39 to 1.32 V *vs* Ag/Ag$^+$ and reduction (or n-doping) peaks in a range of −1.80 to −2.22 V *vs* Ag/Ag$^+$, respectively. Copolymers of pyridine give unique cyclic voltammograms exhibiting p-undoping peaks at potentials much different (about 2−3 V lower) from the corresponding p-doping potentials, and this large difference between p-doping and p-undoping potentials is explained by an EC mechanism. They are converted into semiconductors by chemical and electrochemical oxidation and reduction. Copolymers of thiophene with pyridine and quinoxaline show the third-order nonlinear optical susceptibility χ$^{(3)}$ of about 5×10^{-11} esu at the three-photon resonant wavelength, which is 5−7 times larger than those of the corresponding homopolymers and related to the CT structure in the copolymers.

Introduction

Chemical and physical properties of charge-transfer (CT) complexes have attracted strong interest, and a large number of papers have been published about compounds with the CT structures.[1−3] π-Conjugated polymers have also attracted strong interest and been the subject of many recent papers.[4] Although several papers have recently been published on the preparation and properties of π-conjugated polymers with the CT structure,[5,6] more detailed studies seem to be required for revealing their basic properties.

In this papepr, we report preparation of various π-conjugated polymers with the CT structure and their electrochemical and optical properties (UV-visible, photoluminescence, and nonlinear optical properties). This paper deals with the π-conjugated copolymers constituted of heterocycles. Examples

[†] Research Laboratory of Resources Utilization, Tokyo Institute of Technology.
[‡] NTT Opto-electronics Laboratories, Nippon Telegraph and Telephone.
[§] Gunma University.
[‖] Japan Advanced Institute of Science and Technology.

[⊗] Abstract published in *Advance ACS Abstracts,* October 1, 1996.
(1) (a) Briegleb, G. *Elektronen-Donator Acceptor-Komplexe*; Springer: Berlin, 1961. (b) Foster, F. *Organic Charge-transfer Complexes*; Academic Press: New York: 1969.
(2) (a) Mulliken, R. S. *J. Am. Chem. Soc.* **1950,** *72,* 600. (b) Mulliken, R. S. *J. Am. Chem. Soc.* **1952,** *74,* 811.

(3) E.g., (a) Priyadarshy, S.; Therien, M. J.; Beratan, D. N. *J. Am. Chem. Soc.* **1996,** *118,* 1504. (b) Maslak, P.; Chopra, A.; Moylan, C. R.; Wortmann, R.; Lebus, S.; Rheingold, A. L.; Yap, G. P. A. *J. Am. Chem. Soc.* **1996,** *118,* 1471. (c) Roest, M. R.; Verhoeven, J. W.; Schuddeboom, W.; Warman, J. M.; Lawson, J. M.; Paddon-Row, M. N. *J. Am. Chem. Soc.* **1996,** *118,* 1762. (d) Bryan, C. D.; Cordes, A. W.; Goddard, J. D.; Haddon, R. C.; Hicks, R. G.; MacKinnon, C. D.; Mawhinney, R. C.; Oakley, R. T.; Palstra, T. T. M.; Perel, A. S. *J. Am. Chem. Soc.* **1996,** *118,* 330. (e) Fukuzumi, S. *Adv. Electron Transf. Chem.* **1992,** *2,* 67.
(4) (a) Skotheim, T. A., Ed. *Handbook of Conducting Polymers*; Marcel Dekker: New York, 1986; Vols. I and II. (b) Salaneck, W. R.; Clark, D. L.; Samuelsen, E. J. E. Science and Applications of Conducting Polymers; Adam Hilger: New York, 1990. (c) MacDiarmid, A. G.; Heeger, A. J. *NRL Memo. Rep. (Proc. Mol. Electron Devices Workshop)* **1981** AD-A 05816,208. (d) Bradley, D. D. C.; Mori, Y. In *Electronic Properties of Conjugated Polymers III;* Kuzmany, H., Mehring, M., Roth, S., Eds.; Springer: Berlin, 1989.

are:
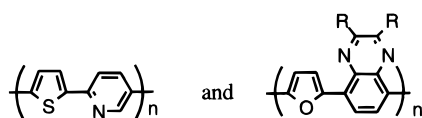
It is established in the chemistry (e.g., in chemical reactivity) of heterocyclic compounds that five-membered ring heterocycles such as thiophene and furan have a π-excessive nature whereas six-membered ring compounds with electron-withdrawing imine (C=N) nitrogens (e.g., pyridine and quinoxaline) exhibit a π-deficient nature.[7] Actually, the electron-donating and -accepting ability of the heterocyclic compounds[8−12] (and also their polymers[4,13,14]) are in the order illustrated in Scheme 1. On these bases, the copolymers are considered to have CT structures such as
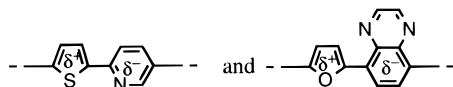
The copolymers reported in this paper are considered to possess linear molecular structures without branching since organometallic polymerization methods applied for the preparation of the copolymers proceed selectively at functional groups of monomers. Due to the CT and linear structure, the copolymers are expected to show interesting and unique chemical and physical properties.

Results and Discussion

Preparation. Polycondensation using a zero valent nickel complex[13,15] gives the copolymers shown in Chart 1 in high yields as summarized in Table 1. The following previously reported[5d] copolymers, PThQx(diph)-PFuQx(diHep), prepared

Scheme 1. Order of π-Electron-Donating and -Accepting Ability of the Monomer Unit

IP/eV	8.89	8.87	8.92	9.25	9.25	9.05
EA/eV	-1.76	-1.15	-0.90	-1.15	-0.62	0.7
$E_{1/2}$(red)/V					-2.15	-1.09

π-accepting (or π-deficient)[7] $\longrightarrow$

IP: ionization potential (in gas phase).[8] EA: electron affinity[9,10]

$E_{1/2}$(red): polarographic reduction potential *vs* mercury pool.[11,12]

by using a Stille reaction[16] are also used in this research for investigation of their structure and optical properties. Application of the type B polymerization to a new monomer (Ar′ = 2-butyl-3-phenylquinoxaline-5,8-diyl) affords a new copolymer PThQx(BuPh), and this copolymer is also used (Chart 2).

On the other hand, random type copolymers shown in Chart 3 have been prepared by using the Ni-promoted polycondensation.

The aforementioned polymerizations give the polymers in high yields (80−100% (Table 1)). Data from elemental analysis and NMR agree with chemical structures of the polymers prepared according to eqs 1−3 (cf. the Experimental Section and supporting information). The composition (*m:n*) of the copolymers prepared according to eq 4 roughly agrees with the feeding ratio of the two monomers (supporting information).

IR and NMR. IR spectra of the copolymers give rise to IR peaks originated from the two aromatic units, Ar and Ar′. However, ring deformation bands of Ar and Ar′ groups often show splitting. For example, the ring deformation band of the pyridine ring of poly(pyridine-2,5-diyl) PPy[13a] at 1584 cm^{-1} is split into two bands at 1592 and 1580 cm^{-1} in PThPy. Carbon−

PPy
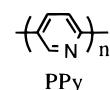
halogen stretching bands of the monomers are not observed in the IR spectra of the copolymers.

^{1}H-NMR as well as ^{13}C-NMR data of the copolymers shown above are reasonable for their structures, (cf. the Experimental Section and supporting information). As shown in Figure 1, ^{13}C{^{1}H}-NMR spectra of symmetrical PPyThPy (chart a) and PPyPhPy (chart c) show a simple absorption pattern with seven peaks, respectively, whereas those of PThPy and PPhPy (chart b) exhibit complicated absorption patterns presumably due to the presence of both the head-to-tail (HT) and head-to-head (HH) units. The ^{13}C{^{1}H}-NMR signals of PPyThPy and PPyPhPy are tentatively assigned as shown in Figure 1 by comparing the ^{13}C{^{1}H}-NMR data with those of known pyri-

(5) (a) Zhou, Z.-H.; Maruyama, T.; Kanbara, T.; Ikeda, T.; Ichimura, K.; Yamamoto, T.; Tokuda, K. *J. Chem. Soc., Chem. Commun.* **1991**, 1210. (b) Yamamoto, T.; Shimura, M.; Osakada, K.; Kubota, K. *Chem. Lett.* **1992**, 1003. (c) Kurihara, T.; Kaino, T.; Zhou, Z.-H.; Kanbara, T.; Yamamoto, T. *Electron. Lett.* **1992**, *28*, 681. (d) Kanbara, T.; Miyazaki, Y.; Yamamoto, T. *J. Polym. Sci. Part A: Polym. Chem.* **1995**, *33*, 999.

(6) (a) Havinga, E. E.; Ten Hoeve, W.; Wynberg, H. *Polym. Bull. (Berlin)* **1992**, *29*, 119. (b) Ferraris, J. P.; Bravo, A.; Kim, W.; Hrncir, D. C. *J. Chem. Soc., Chem. Commun.* **1994**, 991. (c) Karikomi, M.; Kitamura, C.; Tanaka, S.; Yamashita, Y. *J. Am. Chem. Soc.* **1995**, *117*, 6791.

(7) Newkome, G. R.; Paudler, W. W. *Contemporary Heterocyclic Chemistry;* John Wiley: New York, 1982.

(8) (a) Lias, S. A.; Bartmess, J. E.; Holmes, J. L.; Levin, R. D.; Liebman, J. F.; Mallard, W. G. *J. Phys. Chem. Ref. Data Suppl.* **1988**, *17*, 1. (b) *Kagakubenran Kisohen;* Jpn. Chem. Soc. Ed.; Maruzen: Tokyo; 1993, II-620 and II-630. (c) Distefano, G.; Pignatro, S.; Innorta, G.; Fringuelli, F.; Marioni, G.; Taticchi, A. *Chem. Phys. Lett.* **1973**, *22*, 132. (d) Cooper, C. D.; Williamson, A. D.; Miller, J. C.; Compton, R. N. *J. Chem. Phys.* **1980**, *73*, 1527. (e) Johnston, R. A. W.; Melon, F. A. *J. Chem. Soc. Faraday Trans. 2* **1973**, *69*, 1155.

(9) (a) Jordan, K. D.; Burrow, P. D. *Acc. Chem. Res.* **1978**, *11*, 341. (b) Jordan, K. D.; Burrow, P. D. *Chem. Rev.* **1987**, *87*, 557. (c) Nenner, I.; Schulz, G. J. *J. Chem. Phys.* **1975**, *62*, 1747. (d) Modelli, A.; Guerra, M.; Jones, D.; Distefano, G.; Irgolic, K. J.; French, K.; Pappalardo, G. C. *Chem. Phys.* **1984**, *88*, 455.

(10) Janousek, B. A.; Brauman, J. I. In *Gas Phase Ion Chemistry*; Ed. Bowers, M. T.; Academic Press: New York: 1979; Vol. 2, p 53.

(11) Wiberg, K. B.; Lewis, T. P. *J. Am. Chem. Soc.* **1970**, *92*, 7154.

(12) (a) Perichon, J.; Herlem, M.; Bobilliart, F.; Thiebault, A.; Nyberg, K. *Encyclopedia of Electrochemistry of the Element*; Bard, A. J., Lund, H., Eds.; Marcel Dekker: New York, 1978; Vol. XI, p 2. (b) Baumgärtel, H.; Retzlav, K.-J. *Ibid.* 1984; Vol. XV, p 167.

(13) (a) Yamamoto, T.; Maruyama, T.; Zhou, Z.-H.; Ito, T.; Fukuda, T.; Yoneda, Y.; Begum, F.; Ikeda, T.; Sasaki, S.; Takezoe, H.; Fukuda, A.; Kubota, K. *J. Am. Chem. Soc.* **1994**, *116*, 4832. (b) Yamamoto, T.; Morita, A.; Miyazaki, Y.; Maruyama, T.; Wakayama, H.; Zhou, Z.-H.; Nakamura, Y.; Kanbara, T.; Sasaki, S.; Kubota, K. *Macromolecules* **1992**, *25*, 1214. (c) Yamamoto, T.; Sugiyama, K.; Kushida, T.; Inoue, T.; Kanbara, T. *J. Am. Chem. Soc.* **1996**, *118*, 3930.
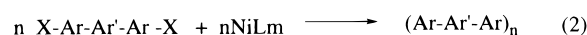
(14) (a) Zotti, G.; Schiavon, G.; Comisso, N.; Berlin, A.; Pagani, G. *Synth. Met.* **1990**, *36*, 337. (b) Wernet, W.; Wegner, G. *Makromol. Chem.* **1987**, *188*, 1465. (c) Yamamoto, T.; Wakayama, H.; Fukuda, T.; Kanbara, T. *J. Phys. Chem.* **1992**, *96*, 8677. (d) Diaz, A. F.; Castillo, J. I.; Logan, J. A.; Lee, W.-Y. *J. Electroanal. Chem.* **1981**, *129*, 115. (e) Dian, G.; Barbey, G.; Decroix, B. *Synth. Met.* **1986**, *13*, 281. (f) Yoshino, K.; Kohno, Y.; Shiraishi, T.; Kaneto, K.; Inoue, S.; Tsukagoshi, K. *Synth. Met.* **1985**, *10*, 319. (g) Yamamoto, T. *J. Polym. Sci., Part A: Polym. Chem.* **1996**, *34*, 997.

(15) (a) Wang, Y.; Quirk, R. P. *Macromolecules* **1995**, *28*, 3495. (b) Kreyenschmidt, M.; Uckert, F.; Müllen, K. *Macromolecules* **1995**, *28*, 4577.

(16) (a) Echavarren, A. M.; Stille, J. K. *J. Am. Chem. Soc.* **1987**, *109*, 5478. (b) Bao, Z.; Chan, W.; Yu, L. *Chem. Mater.* **1993**, *5*, 2.
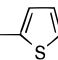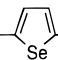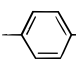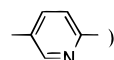
Chart 1

Type A polymerization:

$$n \text{ X-Ar-Ar'-X } + n\text{NiLm} \longrightarrow (\text{Ar-Ar'})_n \qquad (1)$$

$$n \text{ X-Ar-Ar'-Ar -X } + n\text{NiLm} \longrightarrow (\text{Ar-Ar'-Ar})_n \qquad (2)$$

NiLm: zerovalent nickel complex (a mixture of bis(1,5-cyclooctadiene)nickel(0) Ni(cod)$_2$ and neutral ligand (L)).

X: halogene.

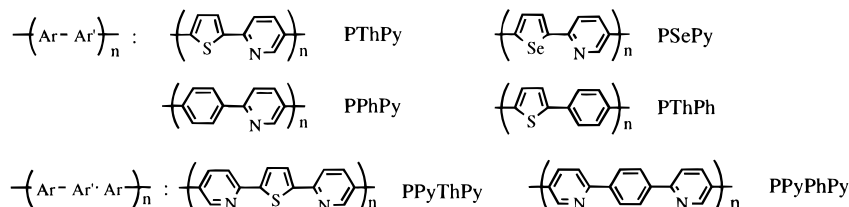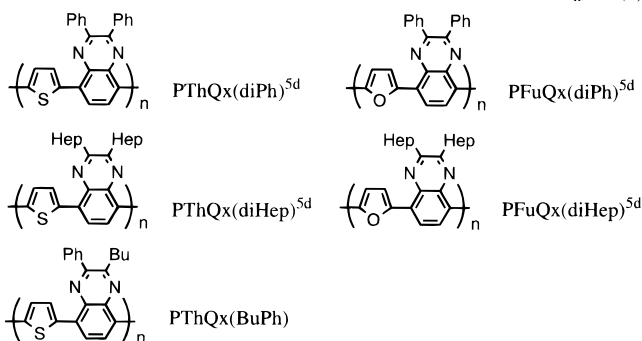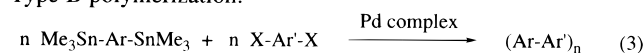Ar, Ar': arylene (Th = ; Se = ; Ph = ; Py =)

$-(\text{Ar}-\text{Ar'})_n-$:　PThPy　PSePy　PPhPy　PThPh

$-(\text{Ar}-\text{Ar'·Ar})_n-$:　PPyThPy　PPyPhPy

Chart 2

Type B polymerization:

$$n \text{ Me}_3\text{Sn-Ar-SnMe}_3 + n \text{ X-Ar'-X} \xrightarrow{\text{Pd complex}} (\text{Ar-Ar'})_n \qquad (3)$$

PThQx(diPh)[5d]　PFuQx(diPh)[5d]

PThQx(diHep)[5d]　PFuQx(diHep)[5d]

PThQx(BuPh)

Ph = phenyl.　　Hep = heptyl.　　Bu = butyl.

dine-, thiophene-, and benzene derivatives[17] as well as with those of 2-(α-terthienyl)pyridine Th$_3$α-Py, 3-(α-terthienyl)pyridine Th$_3$β-Py, and 5,5′-(2-pyridyl)-2,2′-bithiophene α-PyTh$_2$α-Py prepared in this research.

^{1}H-NMR spectra of PFuQx(diHep) and PThQx(BuPh) (charts a and b in Figure 2) also agree with their structures; splitting of the butyl signals of PThQx(BuPh) is attributed to the presence of the HT and HH units with respect to the Qx(BuPh) group.

Molecular Weight, Solubility, and Molecular Structure. PThPy (run 1 in Table 1) has a molecular weight (mw) of 5400 corresponding to the degree of polymerization of 35, as determined by a light scattering method.[18] A large [η] value (2.26 dL g^{-1}) of PThPy for its M_w value is attributed to its stiff structure. PPyThPy (run 9) gives an [η] value of as high as 4.4 dL g^{-1}. In the case of the random copolymers of thiophene and pyridine (PSN13 and PSN11, runs 16 and 17), they have a M_w of 5×10^4–3.3×10^5.

The copolymers containing the pyridine unit are generally soluble in formic acid, whereas the copolymers containing the quinoxaline unit are soluble in CF$_3$COOH. Drying up solutions of the copolymers under vacuum affords the original polymers as proved by IR spectroscopy. Although UV-visible absorption peaks of the copolymers in the acidic solutions show shifts from those in solvent-free films (Table 1), the results indicate that the solvent does not form stable salts with the copolymers and can be removed under vacuum. Sometimes, a small amount of CF$_3$COOH remained in the polymer sample after the drying under the vacuum. However, treatment of the sample with NH$_3$-(aq) followed by drying under vacuum gives solvent-free original polymer.

Introduction of unsymmetrical substituents in the quinoxaline unit [13c] as in PThQx(BuPh) (eq 3) renders the polymer some solubility in nonacidic solvents such as CHCl$_3$ and toluene.

The light scattering measurement reveals that PThPy, PSN13, and PSN11 have the ρ_v (degree of depolarization)[18] values of 0.09, 0.024, and 0.022, respectively, in formic acid. The ρ_v value of PThPy is smaller than that ($\rho_v = 0.33$)[13a] of rigidly linear PPy (*vide ante*); however, the value of 0.09 is comparable to that of a stiff poly(aromatic amide), poly(*p*-benzamide),[18c] and suggests PThPy also takes a rather stiff structure in the solution. The copolymers have large refractive index increments of $\Delta n/\Delta c = 0.53 - 0.69$ cm^3 g^{-1}.

Because of the stiff structure, PThPy molecules in a stretched poly(vinyl alcohol) (PVA) film exhibit a fairly strong dichroism. Similar dichroism was reported for rigidly linear PPy.[13a] The dichroic ratio Rd[13a] observed with the PVA−PThPy film (curve a in Figure 3) is as large as 15 at a stretching ratio R_s of 15; however, it is smaller than that observed with a PVA-PPy film (broken line b in Figure 3) due to a less rigid structure of PThPy.
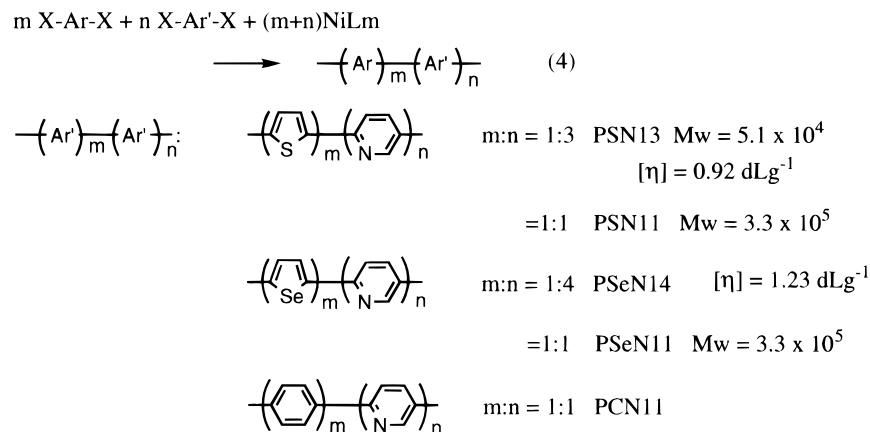
Microstructure and Crystallinity. PThPh, the copolymer of benzene and thiophene, gives rise to sharp powder X-ray 110, 200, and 210 diffraction peaks at $d = 4.5$, 3.9, and 3.1 Å, respectively. It is known that the *p*-phenylene Ph unit in poly-(*p*-phenylene) PPP[19a−c] and thiophene-2,5-diyl Th unit in poly-(thiophene-2,5-diyl)PTh[19d,e] take almost the same crystallographic dimensions. The sharp diffraction peaks of PThPh indicate that it can take a crystalline structure due to the almost the same crystallographic dimensions of the Ph and Th units,

(17) (a) Stothers, J. B. *Carbon-13 NMR Spectroscopy*; Academic Press: New York, 1972. (b) Johnson, L. F.; Jankowski, W. C. *Carbon-13 NMR Spectra*; John Wiley: New York, 1972.

(18) (a) Kubota, K.; Urabe, H.; Tominaga, Y.; Fujime, S. *Macromolecules* **1984**, *17*, 2096. (b) Kubota, K.; Chu, B. *Biopolymers* **1983**, *22*, 1461. (c) Zero, K.; Aharoni, S. M. *Macromolecules* **1987**, *20*, 1957. As for ρ_v, cf. ref 12a.

(19) (a) Kovacic, P.; Feldman, M. B.; Kovacic, J. P.; Lando, J. B. *J. Appl. Polym. Sci.* **1968**, *12*, 1735. (b) Froyer, G.; Maurice, F.; Mercier, J. P.; Riviere, D.1 Le Cun, M.; Auvray, P. *Polymer* **1981**, *22*, 992. (c) Sasaki, S.; Yamamoto, T.; Kanbara, T.; Morita, A.; Yamamoto, T. *J. Polym. Sci.* **1992**, *30*, 293. (d) Mo, Z.; Lee, K.-B.; Moon, Y. B.; Kobayashi, M.; Heeger, A. J.; Wudl, F. *Macromolecules* **1985**, *18*, 1972. (e) Brückner, S.; Porzio, W. *Makromol. Chem.* **1988**, *189*, 961.

Chart 3

$$m\ X\text{-Ar-}X + n\ X\text{-Ar'-}X + (m+n)NiLm$$

eq (4)

m:n = 1:3   PSN13   Mw = 5.1 x 10^4

$[\eta] = 0.92\ dLg^{-1}$

=1:1   PSN11   Mw = 3.3 x 10^5

m:n = 1:4   PSeN14 $[\eta] = 1.23\ dLg^{-1}$

=1:1   PSeN11   Mw = 3.3 x 10^5

m:n = 1:1   PCN11

Table 1. Preparation and Optical Properties of the Donor−Acceptor Copolymers[a]

run	monomer[b]	type[c] of polymerization	ligand or catalyst[d]	% yield[e]	mol wt[f]	ρ_v[f]	$[\eta]$,[g] dL g^{-1}	absorption,[h] λ_{max}, nm (ϵ, M^{-1} cm^{-1}) in solution[h]	film	photo-luminescence,[i] λ_{max}, nm
1	BrThPyBr	A(1)	bpy	100	5.4 × 10^3	0.09	2.26	492 (42000)	475[j,k]	556
2	BrThPyBr	A(1)	PPh$_3$	100	2.3 × 10^3			489		
3	BrThPyBr	A(1)	phen	100	2.3 × 10^3			487		
4	ClThPyBr	A(1)	bpy	100				466		
5	IThPyBr	A(1)	bpy	96				474	477[j]	562
6	BrSePyBr	A(1)	bpy	95				491	485[j]	
7	BrPhPyBr	A(1)	bpy	95			1.9	382 (35000)		
8	BrThPhBr	A(1)	bpy	98					85[l]	
9	BrPyThPyBr	A(2)	bpy	100			4.4	440 (35000)		
10	BrPyPhPyBr	A(2)	bpy	100			2.8	366 (52000)	384[j]	580
11	polymer = PThQx(diPh)[4d]			96			0.37	605 (5000)	603[j]	
12	polymer = PThQx(diHep)[5d]			96			0.47	546 (5000)		
13	polymer = PFuQx(diPh)[5d]			94					692	544[j]
14	polymer = PFuQx(diHep)[5d]			95					601	515[j]
15	Me$_3$SnTh-SnMe$_3$ + BrQx(BuPh)Br	B(3)	Pd(PPh$_3$)$_4$	83			0.43	556	600[j]	634 (721 in film)
16	BrThBr + BrPyBr = 1:3	A(4)	bpy	92	5.1 × 10^4	0.024	0.92	431	407[j]	
17	BrThBr + BrPyBr = 1:1	A(4)	bpy	94	3.3 × 10^5	0.022		471	441[j]	455
18	BrSeBr + BrPyBr = 1:4	A(4)	bpy	80			1.23	360	376	428
								ca. 420sh	ca. 420sh	517
19	BrSeBr + BrPyBr = 1:1	A(4)	bpy	92				363		430
								ca. 420sh		505
								ca. 480sh		
20	BrPhBr + BrPyBr = 1:1	A(4)	bpy	96				362	378	

[a] Polymerization conditions: in *N*,*N*-dimethylformamide; at 60 °C for runs 1−10 and 15−20, at 85 °C for runs 11−14; for 16−24 h. [b] The monomers to give the copolymers shown in eqs 1−4. Th = thiophene-2,5-diyl. Py = pyridine-2,5-diyl. Se = selenophene-2,5-diyl. Ph = *p*-phenylene. Qx(diPh) = 2,3-diphenylquinoxaline-5,8-diyl. Ox(diHep) = 2,3-diheptylquinoxaline-5,8-diyl. Qx(BuPh) = 2-butyl-3-phenylquinoxaline-5,8-diyl. [c] Type of polymerization and the number (in the parentheses) of the corresponding equation (cf. text). [d] Ligand L added in eqs 1, 2, and 4 (bpy = 2,2′-bipyridyl; PPh$_3$ = triphenylphosphine; phen = 1,10-phenanthroline) or catalyst added in eq 3. [e] Based on carbon recovered. [f] Determined by light scattering method. ρ_v = degree of depolarization. [g] Intrinsic viscosity. dL = 100 mL. Solvent: HCOOH for runs 1, 7, 9, 10, 16, and 18; CCl$_2$COOH for run 15; CF$_3$COOH for runs 11 and 12. At 30 °C. [h] Solvent: HCOOH for runs 1−10 and 16−20; CF$_3$COOH for runs 11−14; toluene for run 15. Molecular absorption coefficient (ϵ). sh = shoulder peak. [i] Solvent: the same solvent described in footnote h. [j] Film formed on glass substrate by casting. [k] In PVA film. [l] Vacuum deposited film on glass substrate.

in spite of containing both the head-to-tail HT and head-to-head HH units.

To the contrary, a powder X-ray diffraction pattern of PThPy exhibits only a broad diffraction band due to different crystallographic dimensions between the Th and pyridine-2,5-diyl units,[13a] which make it difficult to make microcrystals of PThPy containing both the HT and HH units.

PThPh

crystalline

PThPy

not so crystalline
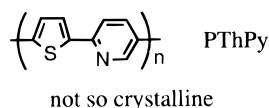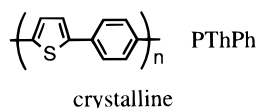
PThQx(diPh) (density = 1.18 g cm^{-1}) gives sharp powder X-ray diffraction peaks at $d = 15.86$ Å/n (15.86 Å, 7.92 Å, 5.29 Å, and 3.94 Å; $n = 1, 2, 3, 4$),[20] which indicate the presence

of one-dimensional order. The distance of 15.86 Å is assigned to the following repeating unit in a monoclinic unit cell based on molecular model and calculation based on the Lennard−Jones potential. Detailed X-ray structural analysis of PThQx-
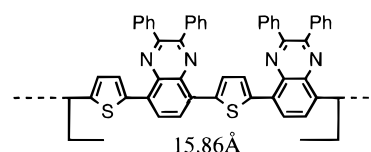
(diPh) agrees with the assignment and will be reported elsewhere. Although the copolymerization expressed by eq 3 is believed to give the alternative copolymer, confirmation of

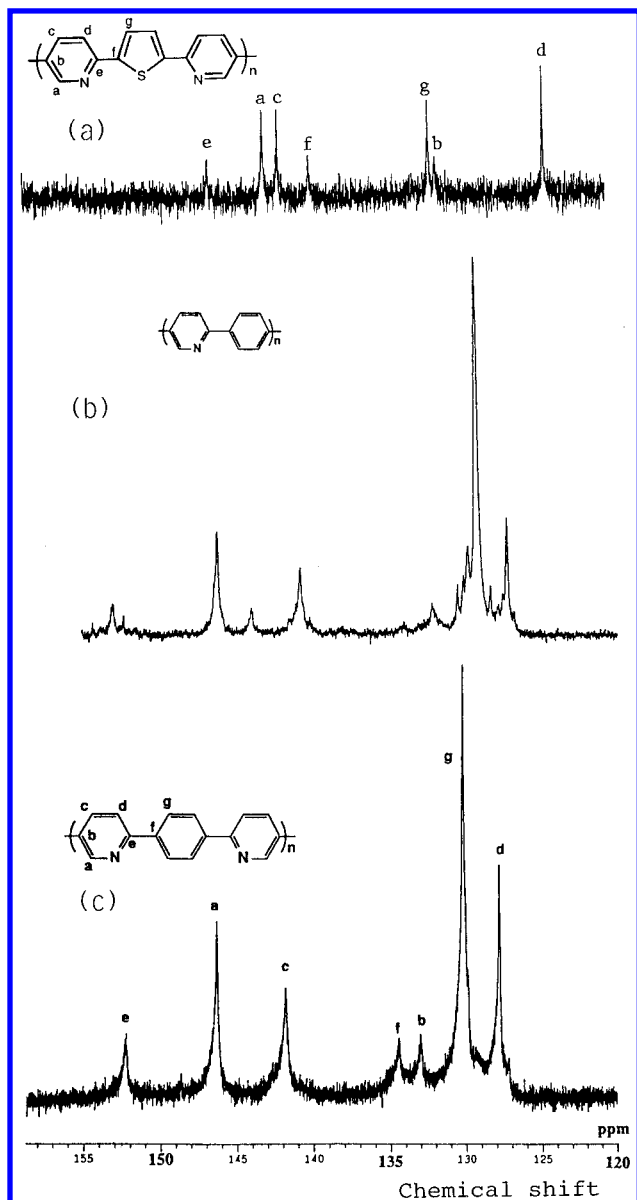(20) Other peaks are observed at $d = 6.53$, 4.70, 4.46, and 3.41 Å.

π-Conjugated Donor−Acceptor Copolymers

J. Am. Chem. Soc., Vol. 118, No. 43, 1996 10393

Figure 1. $^{13}C\{^1H\}$-NMR spectra of (a) PPyThPy, (b) PPhPy, and (c) PPyPhPy in formic acid.
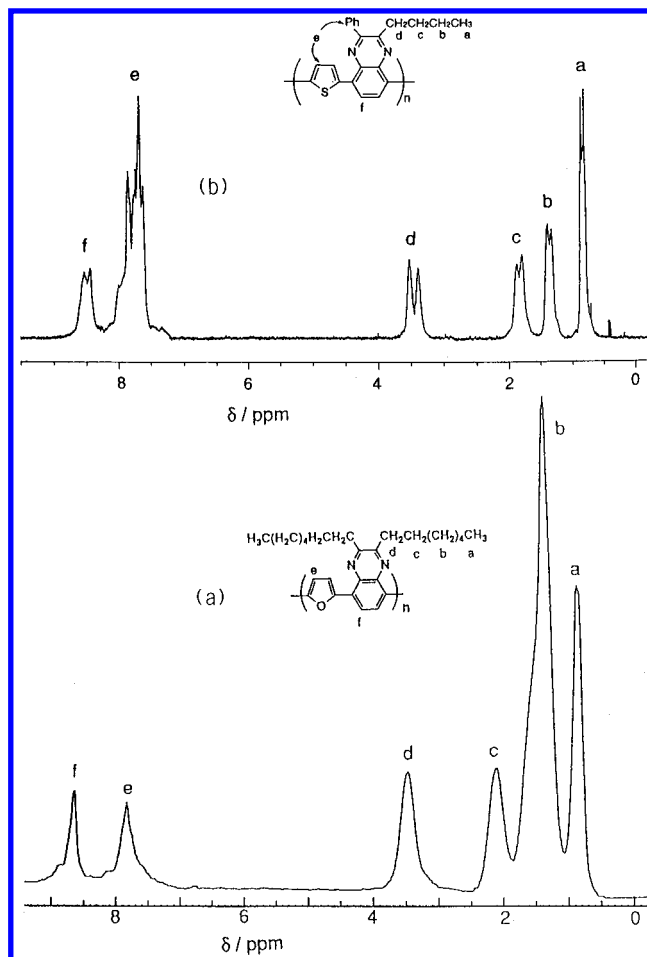

Figure 2. ^1H-NMR spectra of (a) PFuQx(diHep) and (b) PThQx(BuPh) in trifluoroacetic acid-*d*.
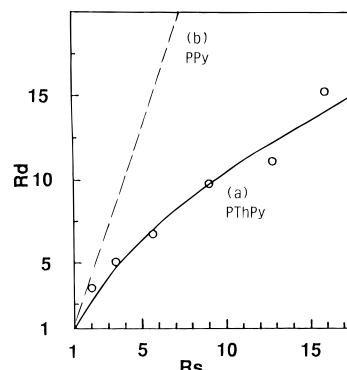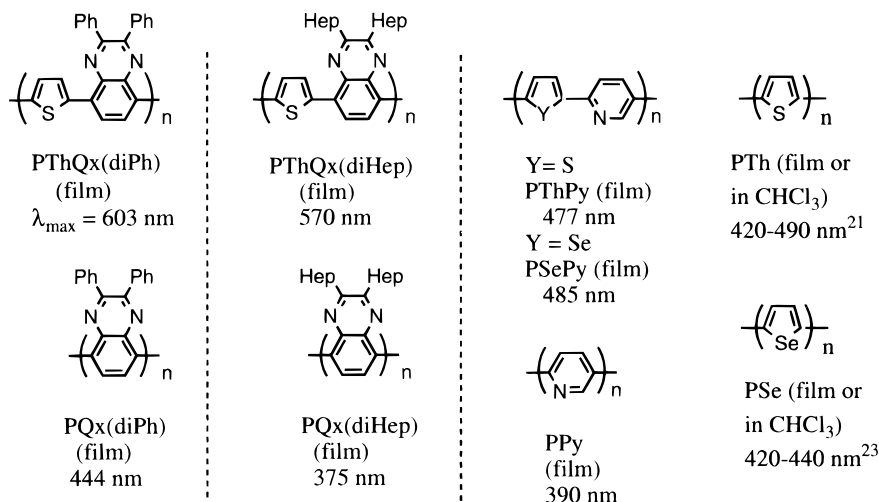

Figure 3. Curve (a): dichroic ratio R_d observed with the lowest energy π−π* absorption band of PVA-PThPy film. Broken line (b): that of the PVA-PPy film.[13a] Definition of the dichroic ratio (R_d) and a stretching ratio (R_s) was given in ref 13a.

this by X-ray crystallography has no precedent.

Optical and Electrical Properties

UV-Visible Absorption. It may be assumed that the copolymer shows its π−π* absorption band at a middle position between the absorption peaks of the corresponding two homopolymers.

However, a solvent-free film of PThQx(diPh) exhibits a UV-visible absorption peak at a longer wavelength ($\lambda_{max} = 603$ nm) than those of films of the corresponding homopolymers PTh ($\lambda_{max} = 420-490$ nm)[21] and poly(2,3-diphenylquinoxaline-5,8-diyl) PQx(diPh) ($\lambda_{max} = 444$ nm).[13c,22] PThQx(diHep), PThPy, and PSePy also give analogous results. Scheme 2 compares the λ_{max} values of the related polymers in the state of solvent-free films (or in CHCl₃).

The appearance of the absorption band of the copolymer at a longer wavelength than the λ_{max} positions of the corresponding homopolymers suggests formation of a unique electronic state related to the postulated CT structure of the copolymers.[24] The dichroism observed with the stretched PVA-PThPy film (*vide ante*; Figure 3) indicates that the π−π* absorption of PThPy has its transition moment essentially along the direction of the polymer chain.

PThQx(BuPh) also shows an absorption peak at a longer wavelength than those of the corresponding homopolymers, PTh

(21) (a) Yamamoto, T.; Sanechika, K.; Yamamoto, A. *Bull. Chem. Soc. Jpn.* **1983**, *56*, 1497. (b) Tourillon, G. In *Handbook of Conducting Polymers*; Skotheim, T. A., Ed.; Marcel Dekker: New York, 1986; Vol. 2, p 293. (c) Okano, M.; Toda, A.; Mochida, K. *Bull. Chem. Soc. Jpn.* **1990**, *63*, 1716. λ_{max} of PTh depends on synthetic methods and conditions for the measurement. Vacuum-deposited PTh thin film[13b] exhibits λ_{max} at 410 nm.

(22) Kanbara, T.; Yamamoto, T. *Macromolecules* **1993**, *26*, 3464.

Scheme 2. Comparison of λ_{max} of Polymer Films

PThQx(diPh)
(film)
$\lambda_{max} = 603$ nm

PThQx(diHep)
(film)
570 nm

PQx(diPh)
(film)
444 nm

PQx(diHep)
(film)
375 nm

Y= S
PThPy (film)
477 nm
Y = Se
PSePy (film)
485 nm

PPy
(film)
390 nm

PTh (film or
in CHCl$_3$)
420-490 nm[21]

PSe (film or
in CHCl$_3$)
420-440 nm[23]

(Scheme 2) and poly(2-butyl-3-phenylquinoxaline-5,8-diyl) PQx(BuPh),[13c] both in the state of a film and a solution in toluene.

PThQx(BuPh)

film
600 nm
in toluene
556 nm

PQx(BuPh)[13c]

film
385 and 340 nm
in toluene
385 and 340 nm
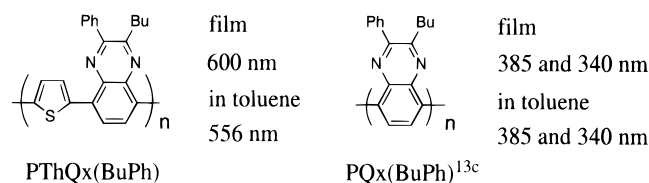
The peak position of PThQx(BuPh) in the film is shifted to a longer wavelength, compared with that in toluene, suggesting the presence of interchain CT interaction in the film in addition to the above discussed intrachain CT interaction. PThQx(BuPh) shows an $[\eta]$ value of 0.43 dL g^{-1} in dichloroacetic acid.

UV-visible absorption bands of films of copolymers of furan also show similar bathochromic shifts from those of the corresponding homopolymers. λ_{max} of a film of poly(furan-2,5-diyl)[25] appears at 468 nm. On the other hand, the UV-visible spectra of the CT polymers, PFuQx(diPh) and PFuQx-(diHep), show the UV-visible absorption peaks at longer wavelengths, 692 and 601 nm, respectively, in the state of film (runs 13 and 14 in Table 1).

MNDO calculation of model compounds H(ArAr')$_3$H and the aromatic monomer units (HArH and HAr'H) indicates that there holds roughly linear correlations for both (i) between the observed $\pi-\pi^*$ transition energy ($E_{\pi-\pi^*}$) of the copolymer and calculated $\pi-\pi^*$ transition energy of the model compound H(ArAr')$_3$H and (ii) between $E_{\pi-\pi^*}$ and energy difference between LUMO of the electron-accepting heterocyclic compound HAr'H and HOMO of the electron-donating heterocyclic compound HArH. The correlation ii is associated with the concept of the CT structure.

A CT structure in a low molecular weight compound, 2-(2'-thienyl)pyridine (ThPy), which corresponds to the repeating unit of PThPy, has been proposed on the basis of its chemical reactivity.[26]
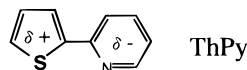
ThPy

By increasing the fraction of pyridine unit from 1/2 (in the case of PThPy) to 2/3 (in the case of PPyThPy), the λ_{max} position

moves in a direction of the λ_{max} position of PPy (run 9 in Table 1). The random type 1:1 copolymers, PSN11 and PCN11 (eq 4), give the absorption bands near those of PThPy and PPhPy, respectively. Increase in the pyridine content (PSN13) leads to shift of the absorption band in the direction of the absorption band of PPy.

As for low molecular weight organic intermolecular CT complexes, occurrence of neutral-to-ionic phase transition is sometimes observed at low temperature as manifested by changes in their UV-visible spectrum.[27,28] However, such a phase transition has not been observed with the present CT copolymers (films) in a temperature range of room temperature through −196 °C.

Photoluminescence. The copolymers of pyridine show strong photoluminescence both in solutions and films, and peak positions of the photoluminescence observed in solutions are shown in Table 1. The peaks of the photoluminescence, except for that of PSeN type copolymers, appear at onset positions of their absorption bands, as usually observed with photoluminescent aromatic compounds. Excitation spectra of the copolymers show peaks at the positions of their absorption peaks. These results indicate that the photoluminescence takes place by migration of electron in a conduction band (π^* level) to a valence band (π level).

Block Structure of PSeN and Energy Transfer. Among the PSN and PSeN type copolymers shown in eq 4, PSN type copolymers seem to have a random sequence whereas the PSeN type copolymers seem to possess a block type structure, as judged from their UV-visible and photoluminescence spectra.

PSN11 shows one UV-visible absorption band (chart a in Figure 4) assigned to a CT absorption band near an absorption band of PThPy. To the contrary, the PSeN type copolymers exhibit three UV-visible absorption bands (charts b and c in Figure 4). Two absorption bands are observed near the absorption bands of the corresponding homopolymers and one near the CT band of PSePy (chart d in Figure 4). These results

(23) A CHCl$_3$-soluble part of PSe prepared by dehalogenation polycondensation of 2,5-dibromoselenophene (cf. eq 1) exhibits λ_{max} at 421 nm. Electrochemically prepared PSe gives λ_{max} at about 440 nm.[14f]

(24) Insertion of a less bulky five-membered ring unit like thiophene may release the steric repulsion in the homopolymer of quinoxaline to contribute to the red shift partly. However, as for pyridine copolymers, such an effect seems to be minor.

(25) Glenis, S.; Benz, M.; LeGoff, E.; Schindler, J. L.; Kannewurf, C. R.; Kanatzidis, M. G. *J. Am. Chem. Soc.* **1993**, *115*, 12519.

(26) Koffmann, T.; Beissner, G.; Mainbaum, R. *Angew. Chem., Int. Ed. Engl.* **1971**, *10*, 740.

(27) (a) Torrance, J. B.; Vazquez, J. E.; Mayerle, J. J.; Lee, V. Y. *Phys. Rev. Lett.* **1981**, *46*, 253. (b) Torrance, J. B.; Girlando, A.; Mayerle, J. J.; Crowley, J. I.; Lee, V. Y.; Batail, P. *Ibid.* **1981**, *47*, 1747.

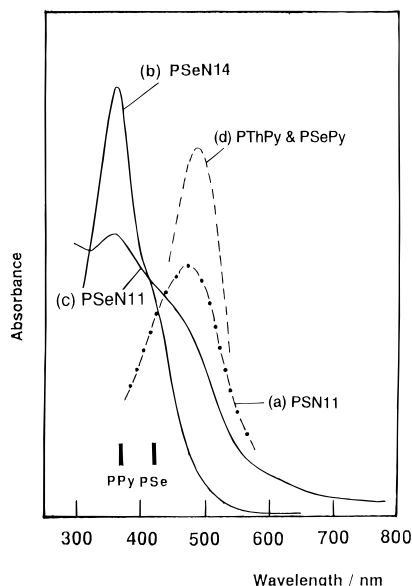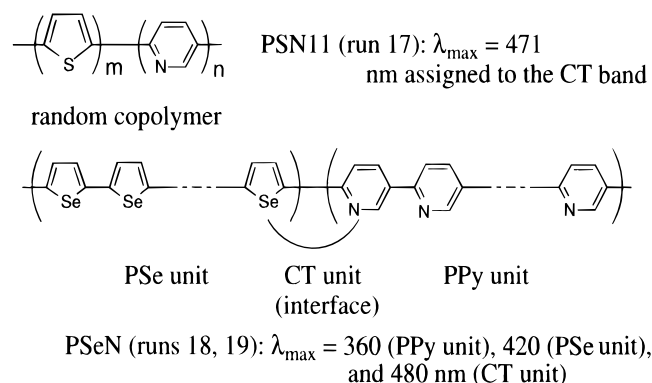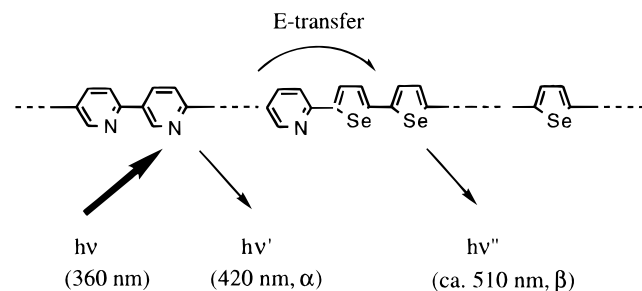(28) Koshihara, S.; Tokura, Y. *Kotaibutsuri* **1992**, *27*, 367.

Figure 4. UV-visible spectra of (a) PSN11, (b) PSeN14, (c) PSeN11, and (d) PThPy or PSePy. PThPy and PSePy give the peak at almost the same position (Table 1). The λ_{max} positions of PPy and PSe are also shown by bars. Solvent: HCOOH for PSeN, PSN, and PPy; CHCl$_3$ for PSe (soluble part).

Scheme 3. Random Structure of PSN11 and Block Structure of PSeN

PSN11 (run 17): λ_{max} = 471 nm assigned to the CT band

random copolymer

PSe unit   CT unit   PPy unit
(interface)

PSeN (runs 18, 19): λ_{max} = 360 (PPy unit), 420 (PSe unit), and 480 nm (CT unit)

Scheme 4. Energy Transfer in Photoluminescence of PSePy

support the random and block structures of PSN and PSeN, respectively. The possibility that PSeN contains the homopolymers, PSe and PPy, is excluded, since PSe is insoluble in formic acid whereas the whole of PSeN14 is soluble in formic acid.

Irradiation of a solution of PSeN with 360 nm light, which induces absorption by the PPy block,[13a] causes appearance of two photoluminescence peaks at positions of light emission from PPy[13a] and PSe.[29]

Detailed examination of the photoluminescence (cf. supporting information), including measurement of excitation spectra

---

(29) PSe[14f] shows a PL peak at 504 nm.

at various modes, suggests occurrence of an energy transfer (E-transfer) from the photoactivated PPy unit to the PSe unit. Such E-transfer has been the subject of recent interest.[30] In contrast to PSeN, PSN gives rise to only one photoluminescence peak (run 17 in Table 1).

Electrochemical and Chemical Redox (Doping) Reaction. Figure 5 depicts cyclic voltammograms (CV's) of a cast PThPy film on a Pt plate. The CV data reveal the following basic electrochemical properties of the film.

(a) In the potential range between −2.4 and 0.6 V *vs* Ag/Ag$^+$ (Figure 5a), the CV curve shows four peaks A−D. The position of peak A corresponds to the oxidation potential of PTh,[4a] and the positions of the C−D couple roughly agree with the doping and undoping potentials of PPy (−2.58 and −2.19 V *vs* Ag/Ag$^+$, respectively).[13a] Color change observed during the electrochemical redox reaction are shown in Figure 5.

(b) In the range −1.95 to 0.6 V, only the A−B couple is observed (Figure 5b), whereas scanning in the range −2.4 to 0 V gives rise to only the C−D couple (Figure 5c).

(c) Both the anodic and cathodic peak currents are essentially proportional to the scanning rate, indicating that the electric current is determined by the mass of PThPy, and the whole of PThPy can participate in the redox reaction due to the conductive properties of the copolymer film.

(d) Use of various electrolytes including [Et$_4$N]X (X = BF$_4$ or ClO$_4$) and [Bu$_4$N]X (Bu = butyl; X = BF$_4$, ClO$_4$ or PF$_6$) affords essentially the same CV curves. CV data of PThPy and other polymers are summarized in Table 2.[31]

These observations indicate that the A−B couple is mainly related to the oxidation (p-doping) and reduction (p-undoping) of thiophene units (eq 5), whereas the C−D couple is mainly related to the reduction (n-doping) and oxidation (n-undoping), of the pyridine unit (eq 6). The positive charge and negative
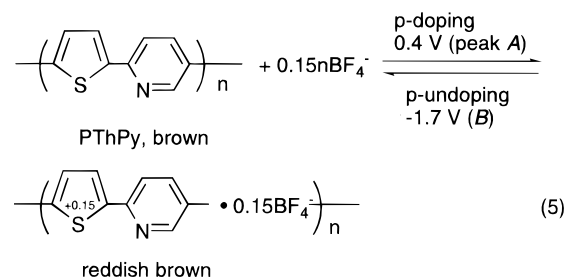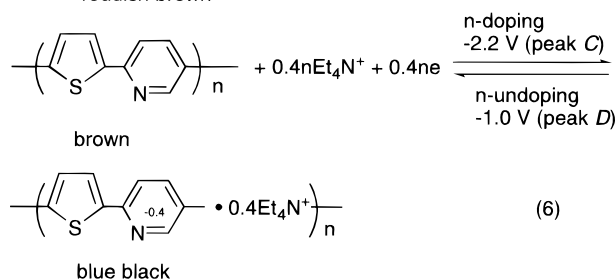
charge formed according to eqs 5 and 6, respectively, are delocalized along the polymer chain; however, they are considered to mainly exist in the thiophene ring and pyridine ring, respectively. The doping level related to eq 5 is ca. 0.15, whereas that related to eq 6 is ca. 0.40, as determined from the electric current.

---

(30) (a) Watkins, D. M.; Fox, M. A.; *J. Am. Chem. Soc.* **1994**, *116*, 6441. (b) Burroughes, J. H.; Bradley, D. D. C.; Brown, A. R.; Marks, R. N.; Mackay, K.; Friend, R. H.; Burns, P. L.; Holmes, A. B. *Nature* **1990**, *347*, 539. (c) Goulle, V.; Harriman, A.; Lehn, J.-M. *J. Chem. Soc., Chem. Commun.* **1993**, 1034. (d) Okamoto, Y.; Kido, J. *Mater. Res. Soc. Symp. Proc.* **1992**, *277*, 65.
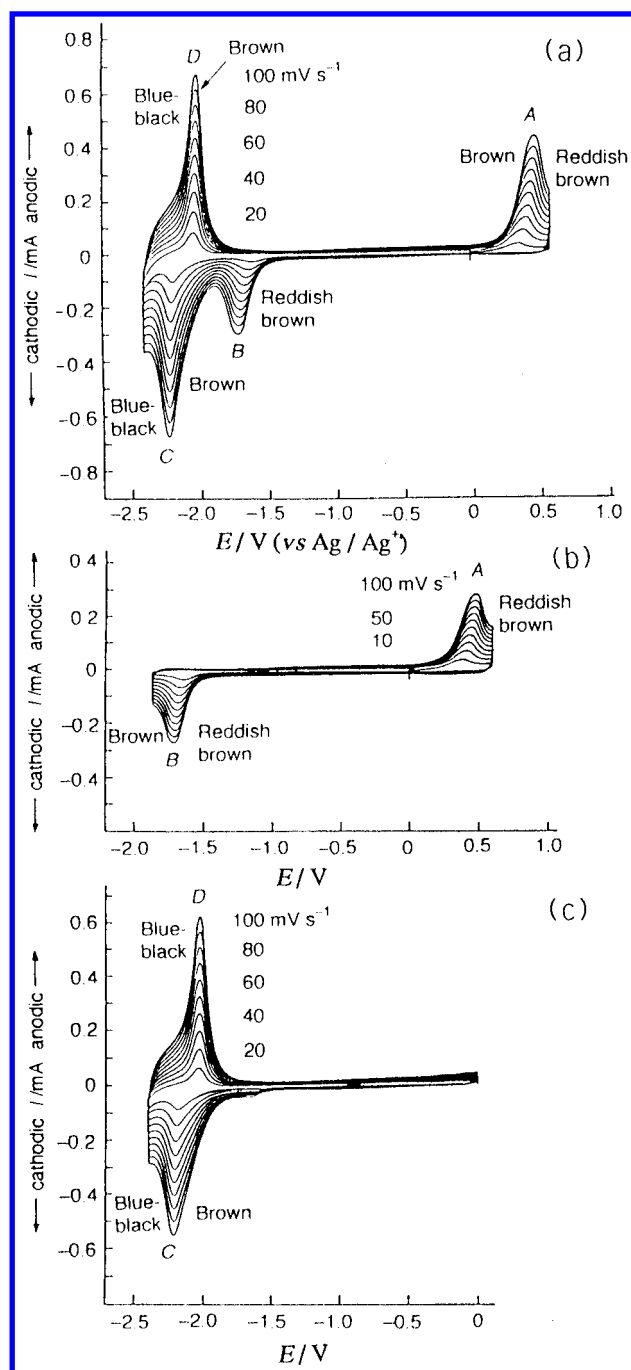
Figure 5. Cyclic voltammograms of a PThPy film (3.8×10^{-8} mol of monomer unit on a 1 cm × 1 cm Pt electrode in a CH_3CN solution of [Et_4N]BF_4 (0.1 M). Potential sweep range (*vs* Ag/Ag$^+$): (a) −2.4 to 0.6 V; (b) −1.95 to 0.6 V; (c) −2.4 to 0 V.

The unusually large potential difference, $\Delta E = E_{pa} - E_{pc} = 2.1$ V, between the A and B peaks of PThPy (eq 5) strongly suggests the occurrence of chemical and/or structural change after the oxidation (peak A) of the thiophene ring (EC mechanism). Since CV charts of 2-(α-terthienyl)pyridine Th$_3$α-Py, 3-(α-terthienyl)pyridine Th$_3$β-Py, and 5,5′-(2-pyridyl)-2,2′-bithiophene α-PyTh$_2$α-Py in solutions show normal redox cycles in both the oxidation and reduction ranges, the unique electrochemical behavior is characteristic of the polymer system in the solid state. Occurrence of a phase transfer due to a change in Coulombic lattice energy caused by the p-doping and/or solvation of the p-doped film seems to contribute, at least partly, to the large difference in the p-doping and p-undoping potentials.

Other copolymers of pyridine exhibit similar CV curves with such large difference in the p-doping and p-undoping potentials

(Table 2). Use of PPyThPy with a higher content of the pyridine unit affords CV curves similar to those of PThPy, showing larger peaks originated from the n-doping and n-undoping of the pyridine unit.

Quinoxaline Copolymers. In contrast to the copolymers of pyridine, the copolymers of quinoxaline give (a) p-doping and p-undoping peaks of the thiophene and furan rings and (b) n-doping and n-undoping peaks of the quinoxaline rings at normal positions without such large difference between the p-doping and p-undoping potentials (nos. 9−13 in Table 2).[5d] These results indicate that such an EC process observed with the copolymers of pyridine does not proceed with the p-doping and p-undoping of the copolymers of quinoxaline.

This distinct difference between the two types of copolymers may be ascribed to the difference in packing structure between the two types of polymers, which will affect the ease of the chemical and/or structural change after the oxidation. Redox behavior of polymer-modified electrode has been the subject of recent interest, and many papers have been published.[32]

The copolymers themselves show low electrical conductivities. Due to the capability to accept both the p-doping and n-doping, their electrical conductivity is raised by chemical doping with iodine (p-doping) and sodium naphthalide (n-doping). The iodine-doped copolymers exhibit the electrical conductivity of 6.6×10^{-9} (PSeN14) through 4.2×10^{-2} S cm^{-1} (PThPh), whereas the sodium-doped copolymers give the electrical conductivity of 6.6×10^{-6} (PSeN11) through 1.2×10^{-3} S cm^{-1} (PThQx(diPh)).

Electrochemically p-doped PThPy show electrical conductivities similar to that of the iodine-doped PThPy. The electrical conductivity of the electrochemically p-doped PThPy exhibits high stability against time, presumably due to the stability of p-doped state because of the large difference in the p-doping and p-undoping potentials. On the other hand, electrochemically p-doped polyalkylthiophene shows a fairly large time-dependent decrease in its electrical conductivity.[33] The electrical conductivity of each sample is given in supporting information.

Optical Third-Order Nonlinear Susceptibility $\chi^{(3)}$. Processable polymer materials with a large $\chi^{(3)}$ are considered to be important materials for rapid switching of light.[4] Since it is known that a narrower band gap of a π-conjugated polymer brings about a larger $\chi^{(3)}$,[4] the shift of the $\pi-\pi^*$ absorption band to the longer wavelength in the present CT polymers is expected to contribute to enhancement of the $\chi^{(3)}$ value. Figure 6a shows UV-visible and $\chi^{(3)}$ spectra of a cast film of PThQx-(diHep), the latter of which are measured by an optical third harmonic generation (THG) method. As shown in Figure 6 and Table 3 (no. 3), PThQx(diHep) film gives maximum $\chi^{(3)}$ of about $\chi^{(3)}_{max} = 5 \times 10^{-11}$ esu at a three-photon resonant region of the polymer [fundamental wavelength $\lambda_f(max) = 1700$ nm; $\lambda_f(max)/3 = 567$ nm; fundamental wavelength λ_f = wavelength of light irradiated against the sample].

$\chi^{(3)}_{max}$ of π-conjugated molecules usually appears at the three-photon resonant region, which means that the $\lambda_f(max)/3$ value corresponds to the position of the $\pi-\pi^*$ absorption band contributing to $\chi^{(3)}$. Actually, the PThQx(diHep) film gives the $\lambda_f(max)/3$ agreeing with the λ_{max} of the $\pi-\pi^*$ absorption (Figure

(31) The A−B couple (Figure 5b) is observable only after the potential is scanned at least once beyond −2.4 V to give the C−D couple.

(32) E. g., (a) Hilman, A. R. *Electrochemical Science and Technology of Polymers*; Linford, R. G., Ed.; Elsevier: New York, 1987. (b) Anson, F. C.; Blauch, D. N.; Savéant, J.-M.; Shu, C.-F. *J. Am. Chem. Soc.* **1991**, *113*, 1922.

(33) Miyazaki, Y.; Yamamoto, T. *Synth. Met.* **1994**, *64*, 69.

Table 2. CV Data of the Copolymers

			redox potential, V *vs* Ag/Ag$^+$ ^{b}			
no.	polymer	electrolyte^a	p-doping (E_{pa})	p-undoping (E_{pc})	n-doping (E_{pc})	n-undoping (E_{pa})
1	PThPy	[Et$_4$N]BF$_4$	0.39	−1.68	−2.20	−2.02
2	PThPy	[Et$_4$N]ClO$_4$	0.40	−1.69	−2.21	−2.01
3	PThPy	[Bu$_4$N]BF$_4$	0.41	−1.70	−2.22	−2.02
4	PSePy	[Et$_4$N]BF$_4$	0.5	−1.6	−2.1	−1.9
5	PPhPy	[Et$_4$N]BF$_4$	1.16	−1.97	−2.49	−2.21
6	PThPh^c	[Et$_4$N]BF$_4$	0.86	*d*	−2.14	*d*
7	PThBpy	[Et$_4$N]BF$_4$	0.66	−1.65	−2.24	−2.03
8	PPhBpy	[Et$_4$N]BF$_4$	1.32	−1.94	−2.36	−2.11
9	PThQx(diPh)^f	[Et$_4$N]BF$_4$	0.64	0.60	−1.80^e −1.94	−1.60 −1.85
10	PThQx(diHep)^f	[Et$_4$N]BF$_4$	0.50	0.35	−2.14	−1.90 −2.15^e
11	PFuQx(diPh)^f	[Et$_4$N]BF$_4$	0.50	ca. 0.5^g	−1.86	−1.77 −1.82^e
12	PFuQx(diHep)^f	[Et$_4$N]BF$_4$	0.35	ca. 0.3^g	−2.08 −2.19	−1.96^e −2.06
13	PThQx(BuPh)	[Et$_4$N]BF$_4$	0.53	ca. 0.42	−1.90 −2.09	−2.01 −1.72
14	PSN13	[Bu$_4$N]ClO$_4$	0.85^f	−1.95	−2.20	−1.98
15	PSN11	[Bu$_4$N]ClO$_4$	ca. 0.6	−1.94	−2.14	−2.03
16	PSeN14	[Et$_4$N]BF$_4$	ca. 1.1	−1.85^e	−2.23	−1.99
17	PSeN11	[Et$_4$N]BF$_4$	0.88	*d*	−2.14	−2.05
18	PCN11	[Bu$_4$N]ClO$_4$	ca. 1.2	−2.00^e	−2.26	−2.06

^{a} Bu = butyl. ^{b} Peak potentials are shown: E_{pa} = peak anode potential; E_{pc} = peak cathode potential. Measured in CH$_3$CN. ^{c} Measured with vacuum-deposited thin film of PThPh on ITO glass electrode due to insolubility of PThPh in solvents. ^{d} The CV curve shows clear p-doping and n-doping peaks; however, the corresponding undoping peak(s) are obscure. ^{e} Shoulder peak. ^{f} Data from ref 5b. ^{g} Broad peak.

6a). PThQx(diPh) and PThPy^{34} films also give similar $\chi^{(3)}$ spectra exhibiting a peak of the λ_f(max)/3 value near the π−π* absorption band.

Table 3 summarizes the $\chi^{(3)}_{max}$ values of thin films of the copolymers and homopolymers. As shown in Table 1, PThPy shows a considerably larger $\chi^{(3)}_{max}$ value compared with those of PTh and PPy (nos. 1, 6, and 7). PThQx(diPh) and PThQx-(diHep) give analogous $\chi^{(3)}_{max}$ values (nos. 2 and 3).

The random copolymers PSN11 and PSN13 give about a half $\chi^{(3)}$ value of PThPy, indicating that the concentration of the donor−acceptor junction in the copolymer strongly influences the nonlinear optical properties. In addition, the λ_f(max)/3 position of the PSN11 film deviates from the λ_{max} position of its π−π* absorption and appears near the λ_{max} position of PThPy as shown in Figure 6b. PSN13 film shows the UV-visible absorption band at a shorter wavelength by 34 nm than that of PSN11 film (runs 16 and 17 in Table 1); however, the PSN13 film gives the same λ_f(max) value of 1400 nm or a λ_f(max)/3 value of 467 nm (nos. 4 and 5 in Table 3). These results indicate that enhancement of $\chi^{(3)}$ for the copolymers of thiophene and pyridine originates from an electronic state corresponding to the π−π* absorption at about 470 nm, which is related to the CT structure in the copolymer. However, revealing the first-excited and second-excited electronic states of the π-conjugated polymer will also be important, since a balance of transient dipole moments between such excited states is also regarded as an important factor to determine $\chi^{(3)}$ as discussed theoretically.^{35}

Conclusion

Organometallic polycondensations give various π-conjugated CT copolymers constituted of electron-donating and electron-

(34) We previously reported a $\chi^{(3)}_{max}$ value of 1.5 × 10^{-10} esu.^{5c} However, this value was obtained at a so-called "backside" mode, which gave a considerably larger $\chi^{(3)}$ value than that measured at the mode adopted in the present study (supporting information).

(35) (a) Guo, D.; Mazumdar, S.; Neher, D.; Stegeman, G. I.; Torruellas, W. In *Organic Materials for Non-linear Optics III*; Ashwell, G. J.; Bloor, D., Eds.; The Royal Society of Chemistry: Cambridge, 1993. (b) Mori, Y.; Kurihara, T.; Kaino, T.; Tomaru, S. *Jpn. J. Appl. Phys.* **1992**, *31*, 896.
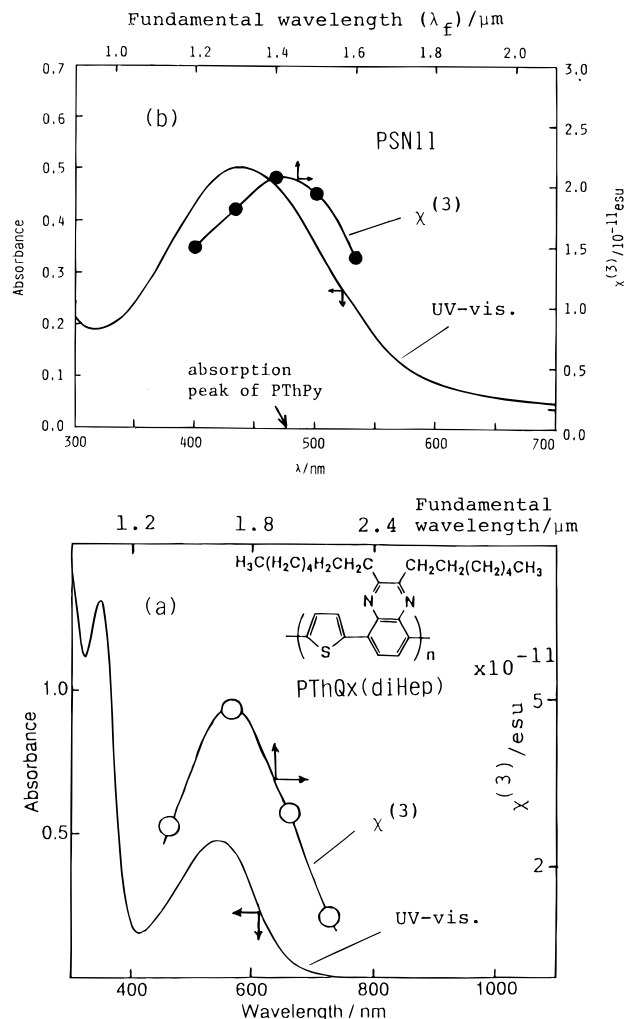
Figure 6. UV-visible and $\chi^{(3)}$ spectra of (a) PThQx(diHep) film (0.079 μm thickness) and (b) PSN11 film (0.054 μm thickness).

10398 *J. Am. Chem. Soc., Vol. 118, No. 43, 1996*

Yamamoto et al.

Table 3. Three-Photon Resonant $\chi^{(3)}$ Values, $\chi^{(3)}_{max}$, of Thin Films of π-Conjugated Polymers[a]

no.	polymer	$\chi^{(3)}_{max} \times 10^{11}$, esu	λ_f(max), nm	λ_f(max)/3, nm
1	PThPy	4.9	1500	500
2	PThQx(diPh)	4.5	1700	567
3	PThQx(diHep)	4.8	1700	567
4	PSN11	2.1	1400	467
5	PSN13	2.5	1400	467
6	PTh[b,c]	0.9	1700	567
7	PPy[b]	0.7[d]		

[a] Maximum $\chi^{(3)}$, $\chi^{(3)}_{max}$, is observed at an irradiated fundamental wavelength of λ_f(max). χ_f(max)/3 is considered to reflect the position of a $\pi-\pi^*$ absorption band contributing to $\chi^{(3)}$. Measured with cast film unless otherwise noted. [b] $\chi^{(3)}$ values for PTh and PPy are estimated from the $\chi^{(3)}$ value measured at a so-called backside mode (cf. supporting information). Corrected $\chi^{(3)}_{max}$ values, which are calculated from relative $\chi^{(3)}_{max}$ values against that of PThPy (no. 1), are given. [c] Measured with vacuum-deposited PTh film.[13b] [d] Value measured at $3\lambda_{max}/\lambda_f$ (or $h\nu/E_g$)[5c] = 0.95.

accepting units. The copolymers exhibit absorption bands at longer wavelengths than those of the corresponding homopolymers. A copolymer, PSeN, having the block-type structure gives rise to the energy-transferred photoluminescence. The copolymers are electrochemically active in both the oxidation (p-doping) and reduction (n-doping) regions, and the copolymers of pyridine exhibit unique p-doping and p-undoping behavior, which can be explained by the EC mechanism. Films of PThPy, PThQx(diPh), and PThQx(diHep) give relatively large $\chi^{(3)}$ values of about 5×10^{-11} esu at their resonant regions, and the relatively large $\chi^{(3)}$ values are considered to be related to the CT structure.

Experimental Section

Materials. Solvents were dried, distilled, and stored under N_2. 2,5-Dibromopyridine, 1,4-dibromobenzene, 2,5-dibromothiophene, 2,2′-bipyridine, triphenylphosphine, *o*-phenanthroline, and 1,5-cyclooctadiene were purchased from Tokyo Chemical Industry Co. Ltd. Ni(cod)$_2$,[13] Pd(PPh$_3$)$_4$,[5d] 2,5-dibromoselenophene,[36] 2,3-diphenyl-5,8-dibromoquinoxaline,[13] 2,3-diheptyl-5,8-dibromoquinoxaline,[13c] and 2-butyl-3-phenyl-5,8-dibromoquinoxaline[13c] were prepared as previously reported. 2,5-Bis(trimethylstannyl)thiophene and 2,5-bis(trimethylstannyl)furan were prepared by modifying a reported method.[37]

Monomers. XThPyBr (X = Cl, Br, and I) was prepared as follows.

ClThPyBr. To a suspension of magnesium turnings (0.224 g, 9.2 mmol) in 5 mL of THF was added 2,5-dichlorothiophene (1.408 g, 9.2 mmol) in 10 mL of THF at room temperature dropwise. Then, the mixture was allowed to stir at room temperature until magnesium turnings were consumed completely (*ca.* 4 h). The produced Grignard reagent was added to a mixture of 2,5-dibromopyridine (2.30 g, 9.7 mmol) and PdCl$_2$(dppb) (0.061 g, 0.10 mmol) suspended in 30 mL of THF at −30 °C dropwise. After the addition was finished, the mixture was stirred overnight from −30 °C to room temperature, and it became a brown homogeneous solution. After THF was removed under reduced pressure, the residue was added to 100 mL of water. The aqueous solution was neutralized by dilute hydrochloric acid and then extracted with benzene (40 mL × 3). The organic layer was washed with water and dried over sodium sulfate. After filtration and concentration, the crude product was recrystallized from 1-propanol. Thus, light yellow crystals were obtained (2,27 g, yield 90%). Mp 108−109 °C. ^{1}H-NMR (CDCl$_3$, ppm): 8.55 (d, 2.2 Hz, 1H, 6-H at Py-ring), 7.77 (dd, 2.2 Hz and 8.5 Hz, 1H, 4-H at Py-ring), 7.42 (d, 8.55 Hz, 1H, 3-H at Py-ring), 7.30 (d, 4.0 Hz, 1H, H at Th-ring), 6.90 (d, 8.55 Hz, 1H, 3-H at Th-ring). ^{13}C-NMR (CDCl$_3$, ppm): Py-ring, 150.5 (6-C), 150.3 (2-C), 139.2 (4-C), 119.1 (3-C), 118.7 (5-C); Th-ring; 142.2 (5-C), 133.0 (2-C), 127.3 (4-C), 124.1 (3-C). UV-vis (THF): λ_{max} = 321 nm. Mass (*m/e*, relative intensity): 227, 275, 273 (M$^+$, 20, 100, 73), 240, 238

(36) Gronowitz, S.; Frejd, T. *Acta Chem. Scand. B* **1976**, *30*, 313.

(37) van Pham, C.; Macomber, R. S.; Mark, H. B., Jr.; Zimmer, H. *J. Org. Chem.* **1984**, *49*, 5250.

([M-Cl]$^+$, 40, 40), 159 ([M − Br − Cl]$^+$, 70). IR(cm^{-1}): 3048, 1572, 1460, 1431, 1208, 1093, 1006, 830, 793, 738. Anal. Found: C, 39.4; H, 1.7; N, 5.2; Br+Cl, 41.8; S, 11.4. Calcd for C$_9$H$_5$NBrClS: C, 39.4; H, 1.8; N, 5.1; Br+Cl, 42.0; S, 11.7%.

BrThPyBr. BrThPyBr was prepared according to the following procedures a and b. Procedure a was similar to the above described procedure for the preparation of 2-chloro-5-(5-bromo-2-pyridyl)-thiophene. The product was separated by column chromatography (silica gel, ether as eluent). Some oligomers and polymer were also produced and separated from BrThPyBr. Yield of BrThPyBr was 20%. Mp 111−112 °C. ^{1}H-NMR (CDCl$_3$, ppm): 8.49 (dd, 0.2 Hz and 0.7 Hz, 1H, 6-H at Py-ring), 7.68 (dd, 2.2 Hz and 8.5 Hz, 1H, 4-H at Py-ring), 7.31 (dd, 8.5 Hz and 0.7 Hz, 1H, 3-H at Py-ring), 7.17 (d, 4.0 Hz, 1H, H at Th-ring), 6.97 (d, 4.0 Hz, 1H, H at Th-ring). ^{13}C-NMR (CDCl$_3$, ppm): Py-ring, 150.8 (6-C), 150.3 (2-C), 139.4 (4-C), 119.4 (3-C), 118.9 (5-C); Th-ring, 145.3 (5-C), 131.3 (3-C), 125.1 (4-C), 115.9 (2-C). UV-vis (THF): λ_{max} = 322 nm. Mass (*m/e*, relative intensity): 321, 319, 317 (M$^+$, 49, 90, 47), 240, 238 ([M − Br]$^+$, 89, 89), 159 ([M − 2Br]$^+$, 100). IR(cm^{-1}): 3046, 1571, 1460, 1424, 1208, 1093, 1007, 831, 791, 738. Anal. Found: C, 34.1; H, 1.6; N, 4.4; Br, 49.8; S, 10.2. Calcd for C$_9$H$_5$NBr$_2$S: C, 33.9; H, 1.6; N, 4.4; Br, 50.1; S, 10.1%.

Procedure b: BrThPyBr was prepared from 2-(5-bromo-2-pyridyl)-thiophene (Minato, A.; Suzuki, K.; Tamao, K.; Kumada, M. *J. Chem. Soc., Chem. Commun.* **1984**, 337). 2-(5-Bromo-2-pyridyl)thiophene (20.23 g, 84.3 mmol) was dissolved in a mixture of acetic acid (150 mL) and chloroform (75 mL), and the solution was cooled to 0 °C in an ice−water bath. Then, to the solution was added bromine (13.4 g, 84.3 mmol) dissolved in 20 mL of acetic acid very slowly (*ca.* 3 h). The mixture was stirred overnight at room temperature, and a large amount of white solid was separated. The solvent (chloroform) was removed under reduced pressure, and the residue was poured into 300 mL of ice−water. After filtration and washing with water, the crude light yellow solid was dried under vacuum and recrystallized from propanol and chloroform (1:1). Thus, white crystals of BrThPyBr were obtained (24.7 g, 92%).

IThPyBr. 2-(5-Bromo-2-pyridyl)thiophene (2.5 g, 10.4 mmol) was dissolved in 15 mL of dichloromethane. Then, iodine (1.4 g, 0.55 mmol) and 4.2 mL of 6 M nitric acid were added. The mixture was refluxed for 2.5 h. After cooling to room temperature, the mixture was poured into an aqueous solution of sodium thiosulfide and extracted with chloroform (40 mL × 4). The organic layer was dried over sodium sulfate and decolored by active carbon. After filtration and concentration, the crude product was recrystallized from acetone to obtain yellow flake crystal (3.6 g, yield 95%). Mp 124−125 °C. ^{1}H-NMR (CDCl$_3$, ppm): 8.57 (d, 2.4 Hz, 1H, 6-H at Py-ring), 7.79 (dd, 8.5 Hz and 2.4 Hz, 1H, H at Th-ring), 7.44 (d, 8.5 Hz, 1H, 3-H at Py-ring), 7.25 (d, 3.9 Hz, 1H, 4-H at Py-ring), 7.19 (d, 3.9 Hz, 1H, H at Th-ring). UV-vis (THF): λ_{max} = 327 nm. Mass (*m/e*, relative intensity): 367, 365 (M$^+$, 100, 100), 240, 238 ([M-I]$^+$, 70, 70), 159 ([M − I − Br]$^+$, 60). IR(cm^{-1}): 3042, 1562, 1448, 1408, 1362, 1093, 1000, 814, 798, 738. Anal. Found: C, 29.8; H, 1.4; N, 3.9; Br+I, 56.1; S, 8.6. Calcd for C$_9$H$_5$NBrIS: C, 29.5; H, 1.4; N, 3.8; Br+I, 56.5; S, 8.8%.

Polymerization. Dehalogenation polycondensations using the zero valent nickel complexes were carried out in manners similar to those previously reported.[13] Copolymers shown in eq 3, except for PThQx-(BuPh), were prepared as previously reported.[5d] PThQx(BuPh) was prepared in an analogus manner.

PThPy. To a solution of bis(1,5-cyclooctadiene)nickel(0) Ni(cod)$_2$ (0.570 g, 2.07 mmol) in 18 mL of dried DMF at room temperature was added 2,2′-bipyridine (0.322 g, 2.07 mmol). After stirring for 1 h, BrThPyBr (0.510 g, 1.60 mmol) was added at once directly to the reaction system. The mixture was allowed to react for 28 h at 60−70 °C. After cooling to room temperature, it was added to 100 mL of 2 M HCl and stirred overnight. After filtration, the reddish brown powder was washed with a mixture of methanol (60 mL) and concd HCl (10 mL), a warm aqueous solution of EDTA (pH = 9, then pH = 3), dilute ammonia, water, and methanol repeatedly, and dried under vacuum for 20 h at 80 °C to obtain PThPy (run 1 in Table 1) (0.261 g, yield = *ca.* 100%). Anal. Found: C, 65.8; H, 3.0; N, 8.2; Br, 1.9. Mw (light scattering) = 5400 calcd for H(Py-Th)$_{33}$Br: C, 66.9; H, 3.1; N, 8.7; Br, 1.5. Mw = 5335 calcd for Br(Py-Th)$_{33}$Br: C, 65.9; H, 3.1; N,

8.5; Br, 3.0. Mw = 5414. IR (cm^{-1}): 1585, 1557, 1525, 1461, 1396, 1384, 1292, 828, 794, 750. ^{13}C-NMR (HCOOH, ppm): 126.0, 129.5, 130.7, 133.3, 133.8, 134.3, 141.0, 143.9, 145.4, 147. CP/MAS ^{13}C-NMR(ppm): 119.5 (relative peak area (RPA) = 1), 128 (RPA = 4.7), 146 (RPA = 3.6), 152.5 (RPA = 1.9). PThPy's prepared analogously from ClThPyBr and IThPyBr, respectively, showed some differences in the IR and ^{13}C-NMR spectra. PThPy from ClThPyBr (run 4): IR (cm^{-1}): 1585, 1558, 1464, 1385, 1333, 1293, 832, 797, 752. ^{13}C-NMR (HCOOH (50 °C), ppm): 125.1, 128.4, 129.7, 130.7, 132.7, 133.0, 135.0, 138.7, 140.6, 142.4, 143.1, 144.6, 146.2. PThPy from IThPyBr (run 5): IR (cm^{-1}): 1585, 1558, 1539, 1525, 1461, 1396, 1340, 1291, 1058, 826, 794, 750. ^{13}C-NMR (HCOOH, ppm): 126.1, 126.4, 129.8, 130.9, 131.4, 133.8, 134.3, 140.8, 142.1, 144.1, 145.1, 146.0, 148.7, 149.0.

PPhPy was prepared in a similar manner. Anal. Found: C, 85.4; H, 4.8; N, 9.1; Br, 0. Calcd for (C$_{11}$H$_7$N)$_n$: C, 86.2; H, 4.6; N, 9.1%. IR (cm^{-1}): 3040, 3010, 1585, 1542, 1457, 815, 754. ^{13}C-NMR (HCOOH, ppm): 127.3, 129.2, 129.8, 130.6, 132.2, 140.9, 144.0, 146.2, 153.0.

Preparation of other polymers using the Ni(0) complex was carried out analogously.

Supporting Information Available: Synthetic and analytical data of monomers other than those described in the Experimental Section, analytical data of polymers other than that described in the Experimental Section, experimental details of measurements, synthetic data of Th$_3$α-Py, Th$_3$β-Py, and α-PyTh$_2$α-Py, table of electrical conductivity of the original and doped polymers, and the photoluminescence spectrum of PSeN14, as well as IR, NMR, powder X-ray diffraction, and thermogravimetric charts of selected polymers (23 pages). These material is contained in many libraries on microfiche, immediately follows this article in the microfilm version of the journal, and can be ordered from the ACS, and can be downloaded from the Internet; see any current masthead page for ordering information and Internet access instruction.

JA961550T